NANO · MICRO small
www.small-journal.com

Pachyrhynchus Weevils Use 3D Photonic Crystals with Varying Degrees of Order to Create Diverse and Brilliant Displays

*Alessandro Parisotto, Ullrich Steiner, Analyn Anzano Cabras, Matthew H. Van Dam, and Bodo D. Wilts**

The brilliant appearance of Easter Egg weevils, genus *Pachyrhynchus* (Coleoptera, Curculionidae), originates from complex dielectric nanostructures within their elytral scales and elytra. Previous work, investigating singular members of the *Pachyrhynchus* showed the presence of either quasi-ordered or ordered 3D photonic crystals based on the single diamond ($Fd\bar{3}m$) symmetry in their scales. However, little is known about the diversity of the structural coloration mechanisms within the family. Here, the optical properties within *Pachyrhynchus* are investigated by systematically identifying their spectral and structural characteristics. Four principal traits that vary their appearance are identified and the evolutionary history of these traits to identify ecological trends are reconstructed. The results indicate that the coloration mechanisms across the Easter Egg weevils are diverse and highly plastic across closely related species with features appearing at multiple independent times across their phylogeny. This work lays a foundation for a better understanding of the various forms of quasi-ordered and ordered diamond photonic crystal within arthropods.

A. Parisotto, U. Steiner, B. D. Wilts
Adolphe Merkle Institute
University of Fribourg
Chemin des Verdiers 4, Fribourg 1700, Switzerland
E-mail: bodo.wilts@plus.ac.at

A. A. Cabras
Coleoptera Research Center
Institute for Biodiversity and Environment
University of Mindanao, Matina
Davao City 8000, Philippines

M. H. Van Dam
Entomology Department
Institute for Biodiversity Science and Sustainability
California Academy of Sciences
55 Music Concourse Dr., San Francisco, CA 94118, USA

B. D. Wilts
Chemistry and Physics of Materials
University of Salzburg
Jakob-Haringer-Str. 2a, Salzburg 5020, Austria

The ORCID identification number(s) for the author(s) of this article can be found under https://doi.org/10.1002/smll.202200592.

DOI: 10.1002/smll.202200592

1. Introduction

The two most common mechanisms for color creation in living organisms are 1) pigmentary coloration involving dye or pigment molecules selectively absorbing specific wavelengths of light and scattering others, and 2) structural coloration with a material possessing a periodic dielectric nanostructure on the length-scale of visible light.[1–3] Materials possessing structural color are often referred to as photonic crystals (PCs) and are characterized by the dimensions/rev displaying in which they possess periodic arrangements. They range from 1D (multilayers or thin films), 2D (arrays of cylinders) to complex 3D PCs.[1] PCs are frequently encountered in nature to endow animals and fruits with brilliant displays. Two common structural coloration mechanisms found in insect structures are multilayers and thin films.[4–6] These endow the insects with bright, angle-dependent colors, and a strong metallic sheen. Structural arrangements lie also at the origin of white scales of certain insects, where multiple scattering by random morphologies reflects light in a broad wavelength range.[7,8] The most complex photonic structures in nature are 3D PCs, whose intricate details are yet to be adequately recreated with man-made, synthetic materials. 3D PCs include gyroid-based minimal surface structures in butterflies[9–11] and birds,[12] as well as diamond-type photonic crystals, which are found within the scales of numerous weevils.[13–16] From a technological viewpoint, the "diamond" structure is particularly interesting as it requires the lowest refractive index (RI) contrast of $\Delta n = 2.1$[17] to create a complete 3D photonic bandgap (PBG). As such high RI contrasts are out of reach for natural materials,[18,19] the reflection of light from a majority of natural PCs is strongly angle-dependent, as they do not possess complete PBGs.

Recently, the scientific focus has shifted away from ordered 3D PCs to photonic structures with correlated disorder, sometimes referred to as quasi-order. These structures have garnered significant attention due to their ability to create angle-independent, stable colors with natural materials, without the need for a complete PBG. These structures have been described in beetles such as *Pachyrhynchus congestus mirabilis*,[20] *Eupholus magnificus*,[21] and *Sulawesiella rafaelae*[22] . Unlike ordered PCs,

quasi-ordered PCs possess only short-range order, that is, they possess a roughly constant nearest-neighbor distance, but no long-range order.

To accurately characterize quasi-order, 3D reconstructions are needed. Previously, X-ray and electron-microscopy-based techniques have been employed to describe these structures.[20,23] Recently, Djeghdi et al. [20] investigated a focused ion beam/scanning electron microscopy (FIB-SEM)-based tomographic reconstruction of the quasi-ordered structures within the elytral scales of a *Pachyrhynchus congestus mirabilis* weevil. This weevil possesses both blue-colored scales based on a quasi-ordered chitinous network as well as red-colored scales incorporating an ordered diamond 3D PC in their wing scales. They showed that both scale types possessed near identical fill fractions and local lattice sizes, hinting at a common developmental origin. However, in-depth knowledge of the genetic and structural background and variations between species of the same family is nonexistent.

Pachyrhynchus weevils are widely renowned for their brilliant and diverse colored markings which function as aposematic signals.[24,25] The weevils are compact, several centimeters in length and feature fused elytra which render them flightless. These weevils are broadly distributed across South-East Asia and are particularly found on the islands of the Philippines, Taiwan, and Indonesia.[26] Their diverse coloration (**Figure 1**), which first drew the attention of entomologists hundreds of years ago (1824, Germar) was only recently reported to be the result of structural coloration.[27] Research on the elytral scales of *P. moniliferus*,[28] *P. congestus pavonius*,[29] and *P. sarcitis*[30] weevils showed the presence of well-ordered diamond-type 3D PCs within their elytral scales. The hue of the rainbow colored scales of *P. congestus pavonius* weevils were shown to arise from modifications in both the fill fraction (*ff*) and the unit cell size of their diamond structure.[29] In a further study investigating the heredity of structural color in *P. sarcitis* weevils, Chang et al. reported that these weevils can also tune their coloration from parent to offspring by varying the orientation of the ordered diamond domains within their scales.[30]

Pachyrhynchus is a speciose genus (with more than 100 species),[26] most of which have yet to be optically or structurally characterized. Here, we investigate the spectral and structural properties encompassing the phylogenetic breadth of *Pachyrhynchus* weevils to identify the main coloration mechanisms in this colorful genus. *Pachyrhynchus* weevils are an excellent study group as their coloration is often confined to bright markings, arranged in spots or lines of a single color. Furthermore, the phylogenetics of this group has recently been studied.[26] To elucidate their photonic properties, the nanostructure of numerous scales were studied using SEM and their spectral properties were measured by microspectrophotometry. These results are combined with phylogenetic data to highlight the plasticity of color generation within this family and to identify areas for further research in the field of biophotonics.

2. Results

Pachyrhynchus weevils display a variety of colorful markings on their 2–4 cm long bodies. Figure 1 shows 12 exemplary specimens each displaying patches, lines or dots with different colors and/or color distributions. To investigate the nature of these brightly colored markings, we characterized the ultrastructure present in the elytral scales of 72 different weevils (see Table S1, Supporting Information), representing the phylogenetic diversity of the genus.[26] These different specimens possess strong differences in the spectral properties of their scales, which arise from variations in the photonic ultrastructures found within them. Below, the various mechanisms giving rise to the diverse and brilliant displays in *Pachyrhynchus* are presented.

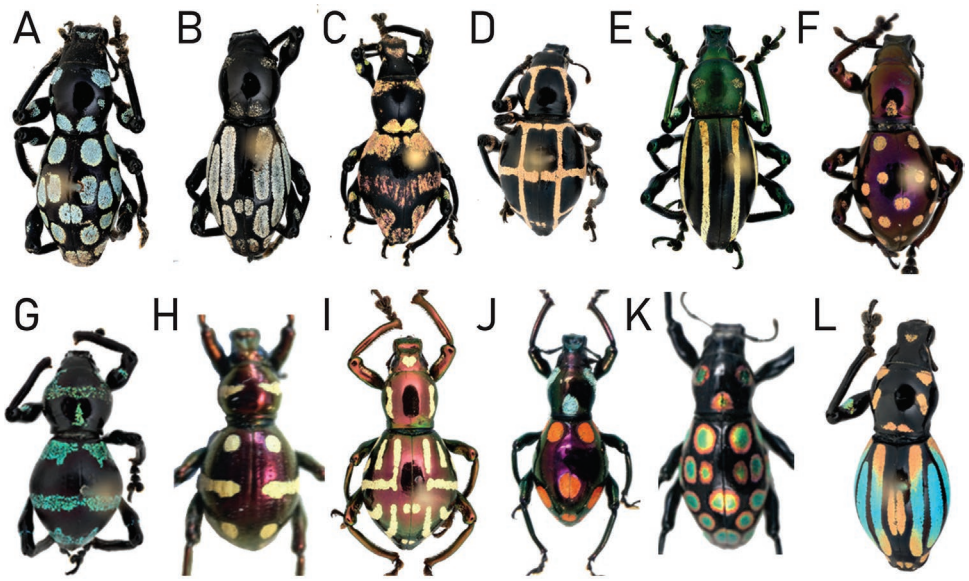

Figure 1. Habitus photographs of various *Pachyrhynchus* weevils. With a size of 2–4 cm, *Pachyrhynchus* weevils are flightless and endemic to oceanic islands of South East Asia. A) *P. lacunosus*, blue variant; B) *P. lacunosus*, white variant; C) *P. niitasoi*; D) *P. mollendorfi marinduquanus*; E) *P. inclytus*; F) *P. confestus*; G) *P. orbifer callainus*; H) *P. elegans*, yellow variant; I) *P. corpulentus*; J) *P. congestus mirabilis*; K) *P. taylori*; and L) *P. barsevskisi*.

2.1. Structural Coloration Mechanisms Vary the Color Appearance of Elytral Scales

Different mechanisms for tuning structural color are observed among *Pachyrhynchus* weevils. Apart from variations in the macroscopic arrangements on their elytral scales, the *Pachyrhynchus* show tremendous variations in the structural properties of the PCs within their scales. These include variations in the short-range order of the 3D PCs within the scales, changes in structural parameters of ordered 3D PCs, as well as variations in the size of the ordered 3D PC domains. Each mechanism has a signature influence on the optical properties of the scales.

2.1.1. Order, Quasi-Order and Disorder in the Photonic Structures within the Elytral Scales

Figure 2 shows the scales and ultrastructures of four exemplary *Pachyrhynchus* weevils that possess different photonic structures within their scales. These include *P. taylori*, *P. inclytus*, and two variants of *P. lacunosus*. The scales of *P. taylori* exemplify the typical optical and structural characteristics of scales arising from ordered 3D PCs. The scales of the blue variant of *P. lacunosus* and *P. inclytus* demonstrate the optical and structural characteristics of quasi-ordered PC structures and the scales of the white variant of *P. lacunosus* show the optical and structural characteristics of scales containing disordered PCs.

A close-up view of the scales on the body of *P. taylori* shows scales that feature a "tessellated" appearance (Figure 2A). The color variations within these scales are attributed to the different orientations of the PCs inside them, which form differently colored domains according to their orientation.[30–32] This is particularly noticeable in the red scales, which possess both red and blue domains. The presence of differently colored domains is a common feature of scales consisting of ordered 3D PCs.[13,21]

To investigate the spectral response of these markings, the reflectance spectra of different colored scales were measured using a custom-adapted microspectrophotometer (see Experimental Section). Figure 2C shows the reflectance spectra of different *P. taylori* scales. In all cases, the reflectance spectra show pronounced reflectance bands, indicating a structural origin of the reflection. To further identify the pigmentary content, single scales were immersed in a refractive index matching oil (n = 1.55, see Figure S1A, Supporting Information). Only trace amounts of a broadband absorbing pigment were found. Although scale colors can vary widely across each marking, the average variation in peak wavelength within unicolored markings or spots averages around 14 nm throughout the species. In samples with varying domain colors, the differently colored domains mix their reflectances to create a color averaging effect creating a nearly monochromatic appearance of the scales.[32,33]

To study the spatial scattering properties of these scales, k-space scattering profiles were measured. Figure 2B shows the resulting scatterograms for narrow- and wide-angle illumination of a red domain within a scale of *P. taylori*. Narrow-angle illumination results in a single colored spot scattered into a narrow spatial angle, indicating that the structure reflects directionally. Under wide-scale illumination, the iridescence of the photonic structure can be visualized,[13] where the reflected colors appear to blue shift with increased observation/incidence angles.

To reveal the structural origin of the reflection, scanning electron microscopy (SEM) was performed. SEM images of the structure within the scales of *P. taylori* (Figure 2D) show that it is highly periodic. The structure closely resembles the <111> orientation of a diamond PC, similar to previous observations from other related weevils.[14–16,28,29] The fast Fourier transform (FFT) image of this image confirms its periodicity and shows a repeating hexagonal pattern (Figure 2D, inset).

The blue-colored scales of *P. lacunosus* (Figure 2E) are very different to those of *P. taylori*. The wing scales possess a single hue and no internal domain structure is visible in the optical micrographs (Figure 2E). Its scales vary from dull to bright blue. The reflectance spectra of these scales, averaged from individual measurements of ten different scales, show that the two scale types are distinctively different: while the bright scales have a peak reflectance of ≈50% at ≈500 nm, the dull scales are blue-shifted to ≈420 nm (Figure 2G) and much less reflective. Both scale types are significantly less reflective than the individual pixelated domains of *P. taylori* shown in Figure 2C. The color of these scales also stems from a nanostructure, as immersion in a refractive index-matching fluid again showed trace amounts of an absorbing pigment (see Figure S1B, Supporting Information). Scatterograms of both scale types (Figure 2F, only dull scales) show that the reflection is angle-independent and that local illumination results in a diffuse reflection. These characteristic differences are indicative of a quasi-ordered nanostructure within their scales[21] and we therefore investigated the scales' interior by SEM. The top view of Figure 2H shows an amorphous-looking structure that lacks periodicity. This is further supported by the featureless FFT of this image that shows a diffuse ring (Figure 2H inset).

The optical properties of the yellow-colored scales of *P. inclytus* (Figure 2I) closely resemble those of *P. lacunosus* as their wing scales possess a single hue and no internal domain structure is visible from optical micrographs (Figure 2I). The reflectance spectra of these scales (Figure 2K) are similar to those of *P. lacunosus*, featuring a broad reflectance band. Their peak reflectance is lowered to ≈622 nm and their FWHM averages around 286 nm. The color of these scales also stems from a nanostructure, as immersion in a refractive index-matching fluid only showed trace amounts of an absorbing pigment (Figure S1C, Supporting Information). Scatterograms of these yellow scales (Figure 2J) show that the reflection is angle-independent and that local illumination results in a diffuse reflection. Their optical characteristics are indicative of a quasi-ordered structure within the scales of *P. inclytus*.[21] The SEM images of Figure 2L show a lack of periodicity and the FFT of this image (Figure 2J, inset) features a distinct, isotropic ring, reflecting the quasi-ordered nature of this structure, with a mean distance of 304 ± 6 nm.

The white variant of *P. lacunosus* possesses white scales (Figure 2M). In beetles, white color has been previously shown to originate from disordered structures within their scales.[7,8] To investigate whether the color of *P. lacunosus* was indeed structural, reflectance (Figure 2O) and transmission spectra

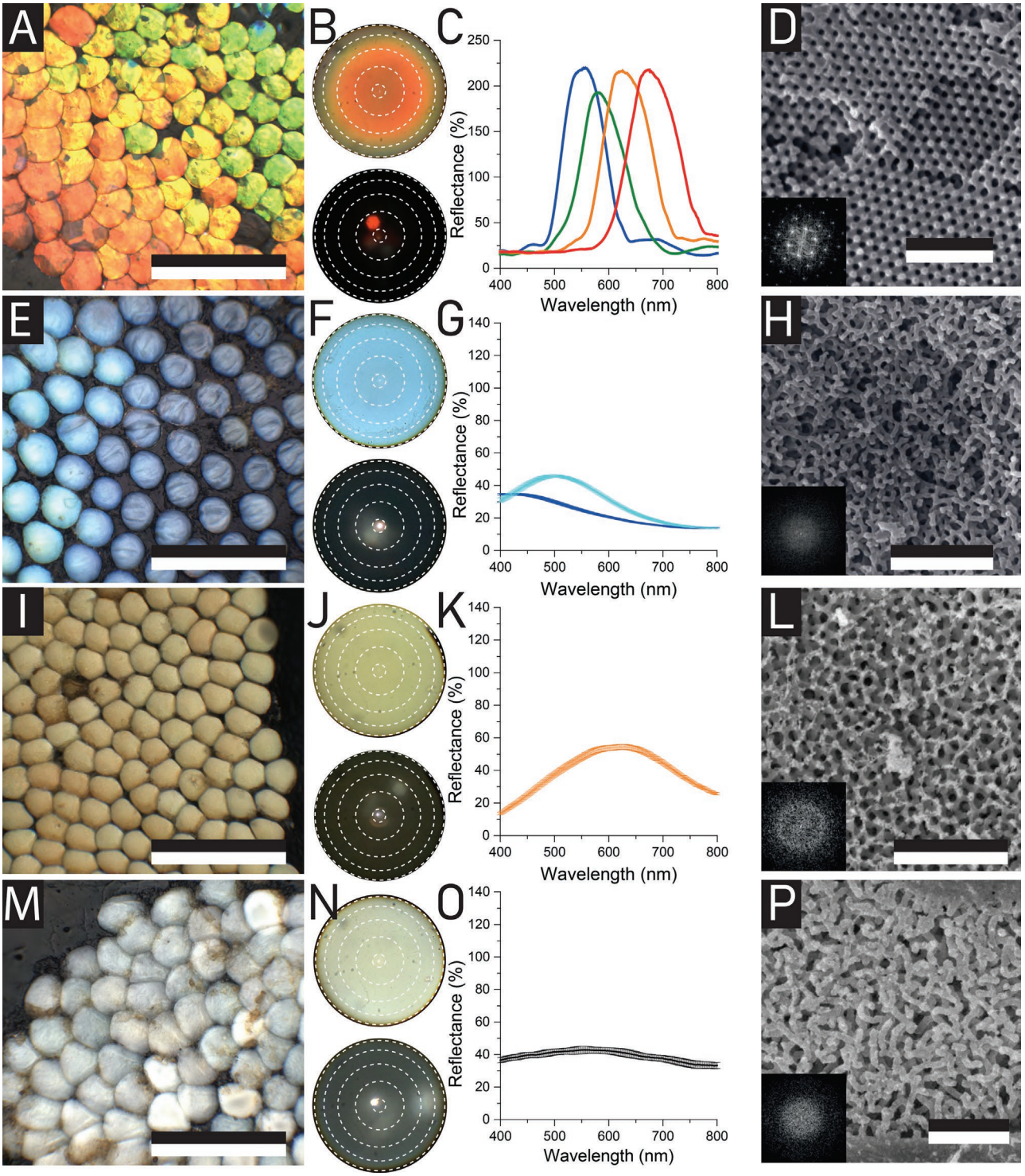

Figure 2. Optical and structural characteristics of A–D) the ordered scales of *P. taylori*, E–L) the quasi-ordered scales of E–H) the blue variant of *P. lacunosus* and I–L) *P. inclytus*, and M–P) the disordered scales of the white (M–P) variant of *P. lacunosus*. A,E,I,M) Optical microscope images. (B,F,J,N) *k*-space images with wide- (top) and narrow-angle (bottom) illumination. The white rings represent scattering angles of 5°, 20°, 35°, 50°, and 65°. C,G,K,O) Representative reflectance spectra (n = 10, mean ± s.e.m). D,H,L,P) Top-view SEM images of the inner scale structures. Insets: 2D-FFT. The structure of (D) *P. taylori* demonstrates a structure resembling that of the [111] lattice of a single-network diamond. Scale bars: (A,E,I,M) 250 µm, (D,H,L,P) 2 µm.

with and without a refractive index-matching fluid were taken of the scales (Figure S1D, Supporting Information). These results show that the white appearance of the scales originates from structural color. The reflectance spectra of the white scales resemble that of a white diffuser, lacking clear reflectance maximum in the visible wavelength range, but with a reflected

intensity of only 30% to 50% relative to a Lambertian white diffuser. Scatterograms (Figure 2R,S) of these white scales also resemble those of a white diffuser. SEM images (Figure 2P) and their FFT (inset) lack the signature of long- or short-range order.

Figure 2 shows that the degree of order in the ultrastructure of the scales strongly influences their optical appearance and their reflected intensity. On the nanoscale level, ordered scales clearly exhibit a periodic structure, whereas the quasi-ordered and disordered scales do not. Based on visual inspection, it appears that the quasi-ordered scales possess a PC structure similar to that of the ordered scales, but with the local unit cells oriented in random directions, with a well-defined nearest neighbor distance. In the disordered scales, no clear nearest neighbor distance is discernible, and the structure is randomly orientated. The optical consequences of this difference are apparent from their reflectance spectra (Figure 2C,G,K,O) and their scattering behavior (Figure 2B,F,J,N). Ordered scales show bright, defined reflectance peaks and directional scattering, quasi-ordered scales have a broader reflectance peak and show diffuse scattering, and white scales exhibit a near-flat reflectance across the visible wavelength range and almost no directional scattering. The difference in order is also manifested in the angle dependence of the structure: it is highly directional and angle-dependent for the ordered scales, while the quasi-ordered and disordered scales scatter light uniformly into a broad angular range. Ordered scales have a brighter reflection, with an almost five-timer higher peak reflectance than that of quasi-ordered scales, which are brighter than disordered scales.

An optical measure enabling a quantitative comparison of order across different structured scales is the FWHM of the reflectance spectra. Ordered scales possess narrow reflectance peaks, with FWHM-values of around 100 nm, while quasi-ordered scales have much larger FWHM-values. For example, the FWHM-values of the bright and dull blue scales of *P. lacunosus* are 212 ± 3 nm and 309 ± 7 nm, respectively, and the FWHM-value of the yellow-scales of *P. inclytus* is 309 ± 7 nm. Disordered scales do not possess an obvious reflectance band, to which no FWHM value can be assigned.

2.1.2. Variations within Order: Structural Parameters

Previous literature has shown that the scale colors of *P. congestus* weevils are tuned through the unit cell size of their PCs (i.e., the PC nearest neighbor distance; see **Figure 3**A) and the filling fraction *ff* of the network morphology within their wing scales.[29] Further studies also showed that the scale color of *P. sarcitis* is controlled by the orientation of the ordered domains within their scales.[30]

To determine whether these mechanisms of color selection are present throughout the genus, the spectral reflectance and ultrastructure of several *Pachyrhynchus* were studied. SEM images were used to determine the nearest neighbor distances (NN) by image analysis (see Experimental Section).The optical characteristics and spectral response of all studied scales were also compared (see Table S2, Supporting Information). This allowed the extraction of the relationship between nearest neighbor distances versus the reflected peak wavelength in weevils with ordered and quasi-ordered scales (Figure 3A). This plot confirms a previous study[29] showing that the peak reflected wavelength varies linearly with the nearest neighbor distance in scales with ordered PCs. Our work not only extends this previous study to the wider *Pachyrhynchus* family, but it also suggests this relationship is present for quasi-ordered PCs. As Maxwell's equations are scale-invariant, this relationship is characteristic for photonic materials, where an increase in the lattice size gives rise to a red-shift of the reflected light, assuming constant RI and *ff* in the scales. Note that the nearest neighbor distance is less well defined in quasi-ordered PCs and is measured by combining FFTs and real space image analysis. Furthermore, natural variations of the NN distance, *ff* and domain orientation within each specimen probably cause the scatter in Figure 3.

While the used procedure can approximate the *ff*, accurate 3D tomographic data for ordered and quasi-ordered scales of *P. congestus mirabilis* weevils exhibited *ff* values of 0.44 and 0.32, respectively.[20] The study of other *Pachyrhynchus* specimens with ordered PCs reported *ff*-values of 0.4, but since they were also based on 2D data, these values are only estimates.[29,30]

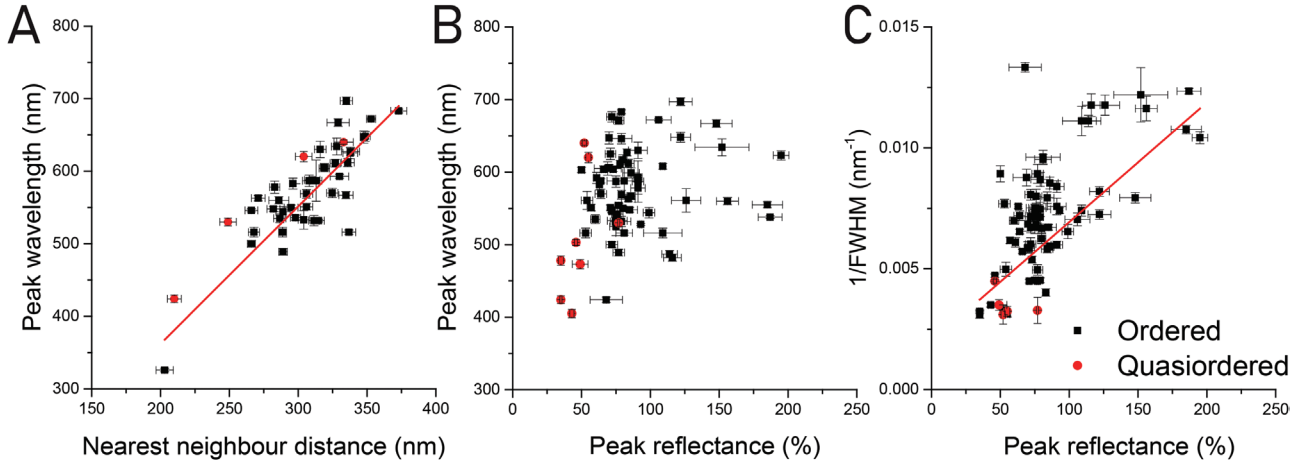

Figure 3. Spectral and nanostructural correlations within *Pachyrhynchus* weevil scales. A) Peak wavelength versus the nearest neighbor distance. A linear fit to the data has a Pearson's *r*-value of 0.89. B) Peak reflectance versus peak reflected wavelength. C) Peak reflectance versus the inverse of the reflection band FWHM. A linear fit to the data has a Pearson's *r*-value of 0.66. Each data point is averaged from 10 measured spectra, error: s.e.m.

Further trends in the optical data were also explored. Although a relationship between reflectance and peak reflected wavelength was not found (Figure 3B), the reflectance and FWHM are roughly inversely proportional (Figure 3C).

2.1.3. Changes in Order: Domain Size Effects

Pachyrhynchus scales containing ordered PCs display a variety of colored domains of different sizes (Figure 2A–D). For a majority of the specimen, these varying domain sizes can only be seen by light microscopy and their scales resemble that of *P. mollendorfi marinduquanus* (Figure 2C), although their color often varies. For these specimens, even though the domains display a variety of colors, their reflectances averages give each scale a specific peak wavelength.[30–32] In most samples, the peak reflectance of the scales within a spot or marking varies by an average of 14 nm. The variation in domain color within each scale is attributed to changes in the orientation of the local PC structure.[30–32]

The different domain size ranges across the species are shown in **Figure 4** in four representative samples of *P. niitasoi*, *P. orbifer callainus P. mollendorfi marinduquanus*, and a yellow variant of *P. elegans*. The analysis of the domain sizes shows a decrease in the average area of differently colored domains from 2300 ± 300. 250 ± 60 and 21 ± 5μ m^2, respectively. The domains of *P. elegans* were too small to be measured accurately, yet vary around 1–3 μm^2 (see Figure S2, Supporting Information). Figure 4A–D shows that domain size variations enable color appearances of the scales ranging from unicolored single domains to assemblies of small domains that are indistinguishable by optical microscopy. These changes

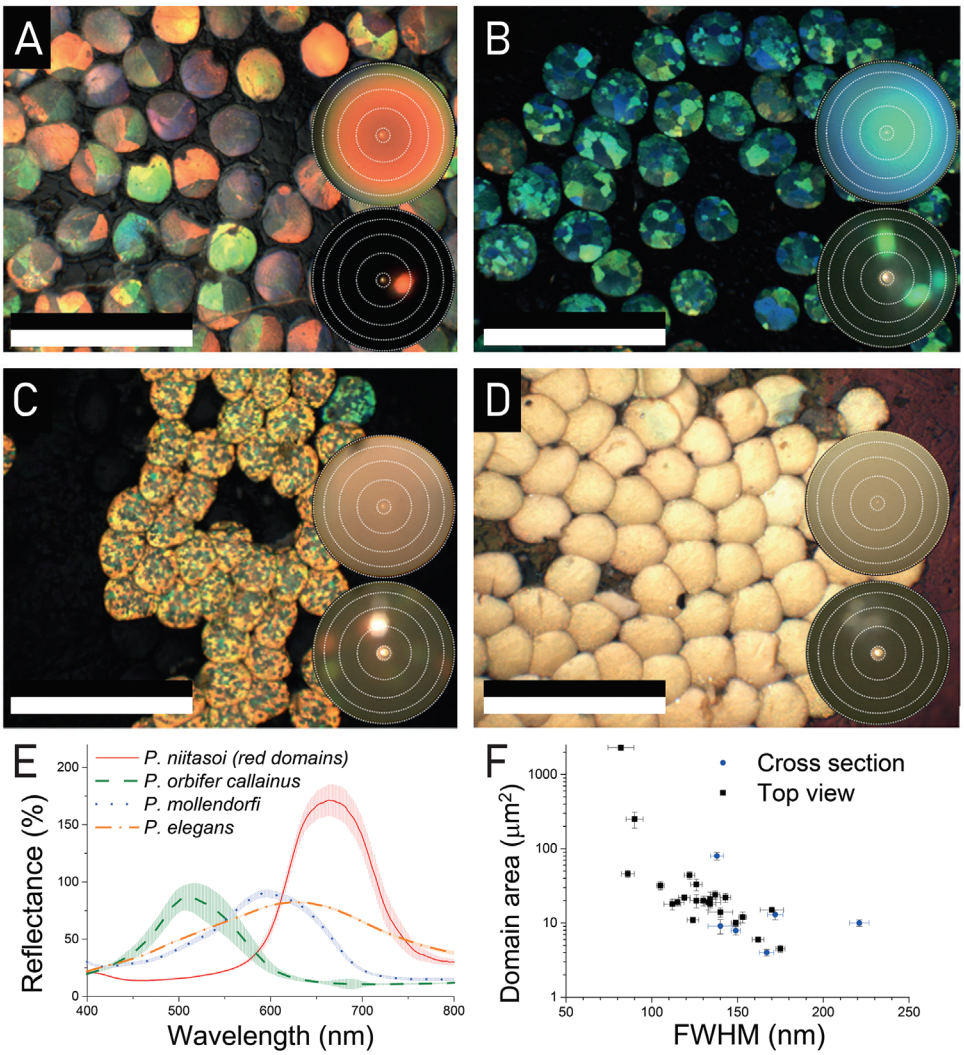

Figure 4. Domain size variations affect the optical appearance. A–D) Optical microscopy images and broad and narrow illumination scatterograms (insets) of the scales of A) *P. niitasoi*, B) *P. orbifer callainus*, C) *P. mollendorfi marinduquanus*, and D) *P. elegans*. The white rings represent scattering angles of 5°, 20°, 35°, 50°, and 65°. The domain areas of each scale were 2300 ± 300, 250 ± 60, and 21 ± 5μ m^2 in (A–C), respectively. The domain size of *P. elegans* was too small to accurately measure. E) Reflectance spectra of the four scale-types (n = 10, error: s.e.m.). F) Domain areas of different *Pachyrhynchus* weevil scales plotted versus the FWHM of their reflectance spectra. The domain areas of the specimen were measured from SEM top-view images (black) complemented by FIB-SEM cross-sections (blue, error: s.e.m.).

in domain size lead to interesting optical variations across the species.

A notable effect of a decreasing domain size is an increase in light scattering , causing enhanced color mixing of the coherently reflected light from the various domains. The effect on an angle-dependent scattering behavior is clearly seen when the scatterograms of the different samples are compared (Figure 4A–D, insets). As the domain size decreases, the reflected light is decreasingly directional and increasingly diffuse. This trend also applies to the reflectance spectra of entire scales (Figure 4E), where decreasing domain sizes leads to increasing FWHM-values, causing decreasing color saturation and reflectance.

It is impossible to accurately resolve the domain sizes by optical microscopy in the majority of the investigated scales. SEM and FIB-SEM analysis were therefore performed to measure the domain sizes and confirm the presence of an ordered crystalline morphology (Figure S2, Supporting Information). To investigate the effect of the domain size on the optical appearance, the average domain area was measured for scales from 29 distinct weevil markings (Figure S2, Supporting Information). An attempt to quantify the optical effects of varying domain size was made, as is shown in Figure 4F, showing a plot of the domain area versus the FWHM of the reflectance peaks of these samples. A decreasing domain size appears correlated with increased FWHM-values. Note, however, that the variance in domain size is significant and that different domains do not always vary in color, as is the case for *P. smaradignus* (Figure S3, Supporting Information). Here, the PCs in the scale are all oriented in the [111] direction, but exhibit in-plane twinning, displaying clear grain boundaries between different domains.

2.2. Variations in Elytral Color

Though less varied than scale colors, the color of the elytron itself which is a single color over the whole body, is another factor involved in the appearance variation of *Pachyrhynchus* weevils. Although the biological function of elytral color is yet to be investigated, it is probably important for aposematic signaling as it provides a contrasting background for the colored weevil scales. Furthermore, the elytron is important as armor, mechanically protecting the weevils from predators.[24]

The majority of the investigated *Pachyrhynchus* weevils possess black elytra (54 of 72 weevils). 12 of 72 weevils featured red elytra and several had pink, purple, or green elytra (6 of 72 weevils). Optical microscopy images of three different elytra colors are shown in **Figure 5**A,D,G. Wide-angle illumination scatterograms show that all but the black colors are angle-dependent. The reflectance spectra of the elytra are distinctly different from the scale spectra and can be categorized into three morphologies (Figure 5B,E,H). The reflection spectra of the black elytron are nearly flat across the visible spectral range with a small increase toward long wavelengths, suggesting the presence of one or more broadband light-absorbing pigments such as melanin.[34] The reflectance spectra of the pink elytron display two clear reflectance peaks at ≈650 nm and at 425 nm (Figure 5E). The shape of this spectrum suggests that the origin of this color is thin film interference.[5] The red elytron has a sharp reflectance peak at ≈650 nm, which is nearly three times brighter and more color saturated (FWHM = 125 nm) compared to the other elytra (Figure 5F). The reflectance spectrum of this elytron resembles that of a multilayer.[4]

To investigate the structural origin of these colors, FIB-SEM on cross-sectional images of these elytra were acquired. The cross-section of the black elytron is featureless, typical of a bulk cuticle.(Figure 5C). The cross-section of the pink elytron features a single, ≈330 nm thick cuticle film on top of the bulk cuticle (Figure 5F), reminiscent of a thin film reflector, giving rise to the calculated spectral characteristics in Figure 5E.

The red elytron exhibits a layered arrangement of electron-dense and -light areas, attributed to chitin and melanin, each about 100 nm thick. Also here, the analytical model shown in Figure 5H closely matches with the experimental spectrum, indicating that this color response arises indeed from multilayer interference.

2.3. Phylogenetics of Color: Ancestral State Reconstructions and Comparative Ultrastructure Analysis

To gain insight into how labile the different types of coloration mechanisms within *Pachyrhynchus* are, the ancestral character states of PC structure was reconstructed via stochastic character mapping (see **Figure 6** and the Experimental Section for details).[26] The results of discrete character model selection favored the equal rates (ER) model as the best fit for our data given the AIC weights (Table S3, Supporting Information).

The results of the ancestral state reconstructions for different scale types show multiple independent transitions between ordered and quasi-ordered/disordered PCs in the elytral scales. A total of nine transitions between ordered and quasi-ordered or disordered nanostructure type in the scales are discernible. In one instance, the scales were first entirely lost in the *P. pinorum* group and subsequently regained as quasi-ordered blue scales in *P. consobrinus*. In several instances, individual weevils possessed several types of nanostructures, as shown in the *P. congestus* species group, where there are two instances of the character states. Interestingly, these two independent origins of the traits also result in different colors of the quasi-ordered PCs. Some species groups however do not seem to show any change from the ordered PC states. For instance, the *P. miltoni* and *P. orbifer* species groups only have ordered PCs despite having a wide range of colors.

Phylogenetically independent contrasts (PICs) (average peak wavelength vs. lattice parameter, average peak wavelength vs. reflectivity, reflectivity vs. FWHM) were studied using a linear model to test for correlations between the variables. The PICs showed that average peak wavelength versus the lattice parameter were strongly correlated, whilst only a weak correlation was found between reflectivity versus FWHM.

3. Discussion

The optical properties of 72 *Pachyrhynchus* weevils were characterized alongside the ultrastructure of 53 different

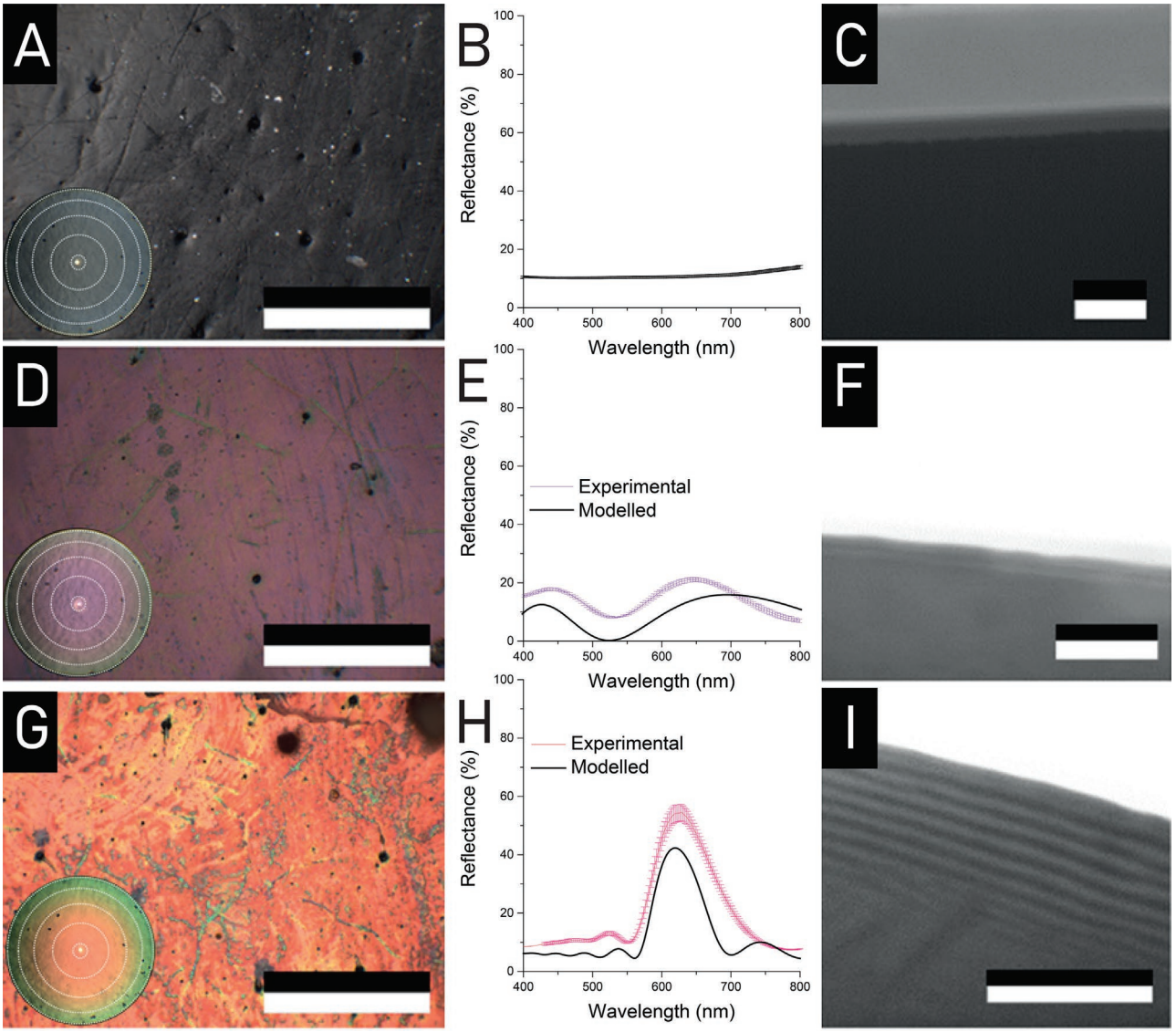

Figure 5. Optical microscopy image and reflectance spectra of the elytra ($n = 6$, mean ± s.e.m.) of A) *P. barsevskisi* (black), D) *P. mirabilis* (pink), displaying thin film interference, G) *P. corpulentus* (red) displaying multilayer interference. Inset: *k*-space reflection images under wide-angle illumination. The white rings represent scattering angles of 5°, 20°, 35°, 50°, and 65°. B,E,F) Reflectance spectra of the elytra corresponding to (A), (D), and (G). C,F,I) Cross-sectional images of the elytra corresponding to (A), (D), and (G). In (C), the top grey layer is a platinum coating and the bottom dark grey thick layer is the elytron. No nanostructure is visible. In (F), a thin film atop the unstructured elytra with a thickness of 310 ± 5 nm is visible. In (I), alternating light and dark-grey layers with an approximate thickness of 100 nm are visible—reminiscent of melanin and pigment-free chitin in other beetle elytra.[4] The structural parameters of (F) and (I) were used to model their reflectance, which are included in (E), and (H), respectively. Scale bars: (A,D,G) 250 µm, (C,F,I) 2 µm.

specimens across the phylogeny. Through this study, we have identified four principal mechanisms with which the studied *Pachyrhynchus* species vary their optical appearance: i) through changes in the 3D PC structure within the scales, encompassing ordered, quasi-ordered and disordered structures (Figure 2), ii) through variations of structural parameters within ordered 3D PC scales (Figure 3), iii) variations in the size of the PC domains within the scales (Figure 4 and Figure S2, Supporting Information), and iv) changes in the mechanism of elytral coloration (Figure 5). We find that the quasi-ordered/disordered traits are rather labile within the genus, with no one clade showing strong phylogenetic clustering for these PC types.

3.1. Order and Disorder

Pachyrhynchus weevils are an ideal species to study variations in structural coloration, not only because of their vast color palette extending from deep-red to the UV, but also because of their ability to create both ordered and quasi-ordered 3D PCs.[20] Although ordered and quasi-ordered 3D PCs within a single specimen have previously been reported,[21,22]) these ordered and quasi-ordered scales were differently colored and located in distinct sections of the elytron. Furthermore, these previously investigated species lack the vast range in colors found across *Pachyrhynchus*. For example, in *Eupholus magnificus*, the

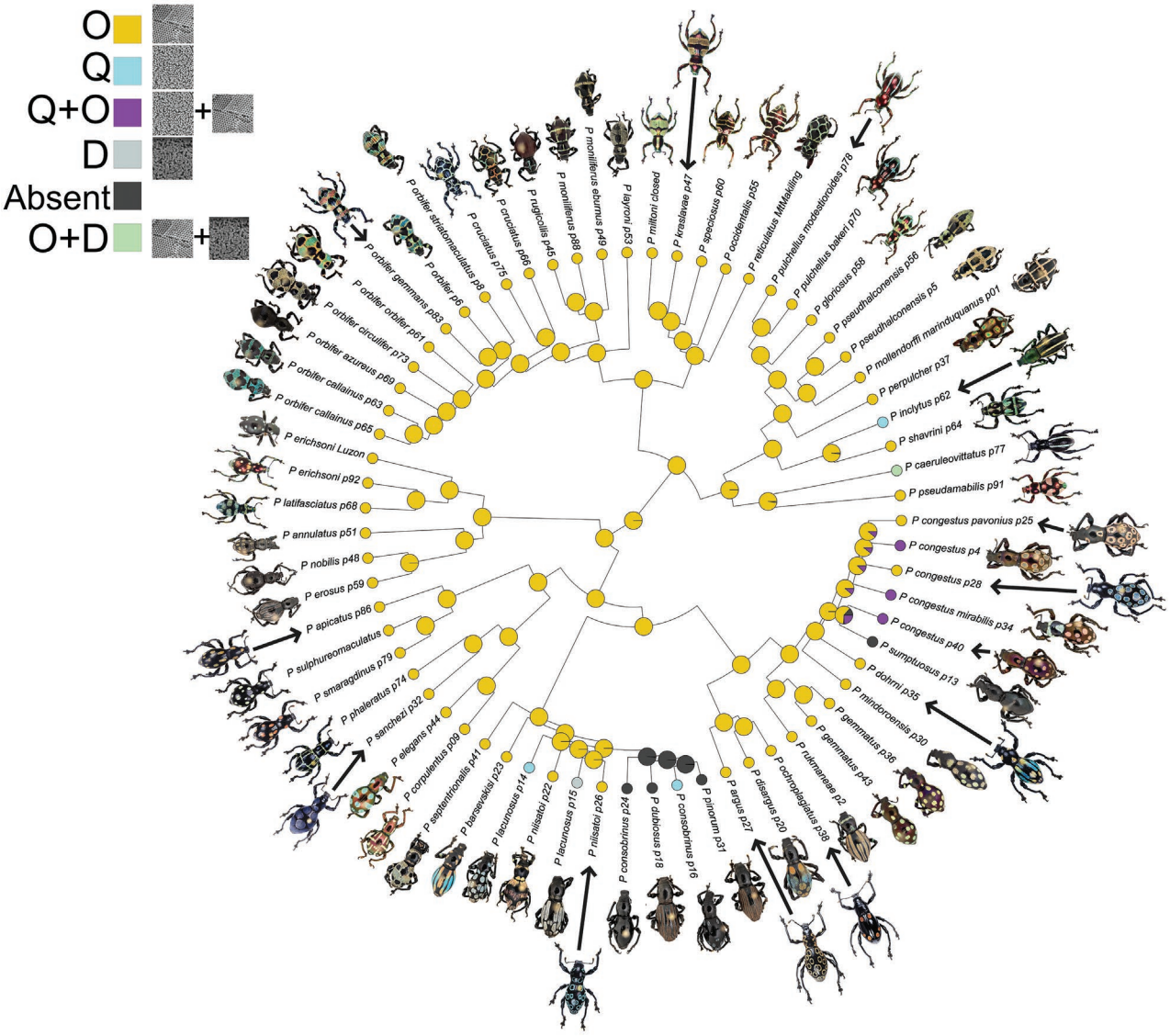

Figure 6. *Pachyrhynchus* phylogeny with ancestral character state reconstructions of the photonic crystal (PC) types. For the scale trait data used in the analyses, (see Tables S1 and S2, Supporting Information).

quasi-ordered structures are only found in the blue scales of the specimen, whereas the ordered scales appear yellow.[21] In contrast, our study shows that the *Pachyrhynchus* can create a vast array of colors with ordered scales alone, extending from the UV to the red (Figure 3) as well as with quasi-ordered structures, which reflect in blue, cyan, yellow and red (Figure 2 and Figure S4, Supporting Information).

Particularly, quasi-ordered and ordered structures in the *Pachyrhynchus* can reflect similar colors and no obvious correlation between color and order exists within the *Pachyrhynchus*. As in photonic glasses, an increase in the size of the scattering unit in quasi-ordered specimen leads to a red-shifted peak reflectance (Figure 3,[35,36]). Yet, it is difficult to create isotropic red colors in photonic glasses as they are typically accompanied by an additional reflectance peak in the blue, leading to color mixing that compromises the red hue.[35,36] Although photonic glasses are different from the quasi-ordered PCs found in the *Pachyrhynchus*, both are quasi-ordered systems. It is therefore interesting that the *Pachyrhynchus* overcome the additional blue reflectance of photonic glasses through the addition of a UV-blue absorbing pigment in the red-reflecting quasi-ordered scales (Figure S4C, Supporting Information).

In addition to quasi-ordered scales, white disordered networks have also been identified in *P. lacunosus*, *P. niitasoi*, and *P. caeruleovittatus* (Figures 2P–T and 6), which possess near flat reflectance spectra over the entire spectral range. Although much brighter disordered structures have been reported in other beetles[7,8,37] these findings do show that the color traits of *Pachyrhynchus* are plastic enough to enable the expression of disordered, quasi-ordered, and ordered PCs. As ordered and quasi-ordered structures can often be found in the same elytral spots (Figure S4A, Supporting Information) and *P. caeruleovittatus* possesses both white disordered and blue ordered scales, we speculate that ordered, quasi-ordered,

and disordered morphologies may develop through a similar process.

Unfortunately, little is known about the development of diamond structures in weevil scales. The development of a topologically related 3D PC, the gyroid, is however better understood in butterflies, where these structures have been reported to develop via the templated self-assembly of an in-folding smooth endoplasmic reticulum membrane, followed by deposition of chitin into the extra-cellular space.[11,38–40] A close look into the in vivo development pathway of these structures is needed and the presents study suggests that *Pachyrhynchus* weevils may be an ideal model for such a study. As breeding of several *Pachyrhynchus* specimens has been successful,[30,41] an extension of these studies may lead to the discovery of the hereditary character of mixing specimens possessing quasi-ordered scales with those who possess ordered diamond scales.

As the markings on the *Pachyrhynchus* are reportedly aposematic,[24,25] it is of interest to determine whether quasi-ordered scales offer a biological function that ordered scales cannot provide, particularly since the same colors can be created by both strategies. Our study shows that the differences between the quasi-ordered and ordered scales lie in changes in iridescence and reflected brightness (Figure 2). There is evidence that the markings may not serve an aposematic function, but that contribute to deterring predation.[42] This theory is supported by the existence of several *Pachyrhynchus* weevils that possess transparent scales or no scales at all, such as *P. sumptuosus*. Quasi-ordered and disordered scales may therefore perhaps not serve a specific biological function and may simply be a part of the development process of diamond PC structures (*vide supra*). Many species occurring in sympatry however converge on scale patterning and the ecological function of the scale coloration (or lack thereof) may therefore be regionally specific.[24]

3.2. Variations in Structural Parameters

Our observations that ordered, diamond-structured scales vary their color by adjusting FF and NN distance agree with previous reports.[29] The linear relationship between peak wavelength and nearest neighbor distance is present throughout the entire genus (Figure 3A) for both ordered and quasi-ordered PCs, which is also supported by these traits phylogenetic independent contrasts.

To better understand the propagation of light through diamond photonic crystals and color-selection effects within the *Pachyrhynchus*, several spectral and structural parameters were compared, including the NN-distance, the peak reflected wavelength, the FWHM of the peak reflectance, the domain size and average reflectivity, to identify relevant correlations.

Given that the refractive index of chitin decreases with reflected wavelength,[43–45] the refractive index contrast should decrease with wavelength and it is expected that a decrease in reflectance would be found as the reflected wavelength increases.[46,47] However, our studies show zero correlation between the measured reflectance and the peak wavelength for the ordered specimen (Figure 3B). Though a correlation between reflected wavelength and peak reflectance is apparent for the quasi-ordered specimen, the Pearson's "*r*" value of the fit is equal to 0.52 and the sample size is too small for this correlation to be given serious significance, especially considering that the peak reflectance values for quasi-ordered specimen show little variation.

However, an inverse relationship was found between the FWHM of the reflectance spectra and their peak reflectance (Figure 3C). While the origin of the relationship is unclear, we speculate that it may arise from defects within the diamond 3D PCs, which would lead to a decreased quality of the 3D PBG, leading to a decreased brightness and broader reflectivity. This relationship appears to occur as the scales transition from ordered to quasi-ordered morphologies.

3.3. Changes in Domain Size

One parameter known to affect the appearance of the *Pachyrhynchus* is their domain orientation,[30] as the optical band gap of diamond 3D PCs varies with their orientation.[13,48] The combination of multiple, differently oriented domains endows the scales with a pointillist effect, which can create nearly angle independent colors.[16,33] In the case of the *Pachyrhynchus* weevils, a change in 3D PC orientation is employed for color tuning without altering the FF or the NN-distance.[30]

The large number of studied specimens enables the study of the appearance of various specimens with varying domain size, thereby improving the understanding of this color mixing effect. With decreasing domain size in the scales of the *Pachyrhynchus*, color mixing is amplified and the iridescence of the scales decreases (Figure 4). This effect is most notable in *P. elegans* of Figure 4D,E, where the domains are so small that they can only be resolved by electron microscopy (Figure S2D, Supporting Information). These small domains create color mixing similar to quasi-ordered scales (Figure 2L), but exhibit a greater reflectance than the latter at similar reflected colors (80% versus 60–40% against a white diffuser standard). This may offer a method of creating bright isotropic colors without necessitating a full PBG.

A decrease in the domain size also appears to increase the FWHM of the scales' reflectance (Figure 4F). Although variations in the domain sizes within each scale and each specimen make it difficult to determine an accurate empirical relationship between the two, it can be seen that domain size influences the optical characteristics of the different specimens, however, an in-depth theoretical modeling approach may be required to accurately predict the relationship between the two. Our data do suggest however the existence of a link between ordered and quasi-ordered specimens (Figure 3C), where samples with smaller domain sizes exhibit a greater amount of disorder in their PC structure, which may be responsible for the increased FWHM values and the decreased reflectance.

3.4. Elytral Colors

The elytral color in the *Pachyrhynchus* stems from three primary coloration mechanisms. The first is pigmentary absorption, which results in black elytra and arises from the lack of any structure on the elytra of black weevils. The second mechanism

is thin film interference, where a thin, transparent film covers the black-colored elytron. This gives rise to thin-film interference, causing a variety of different colors such as pink, purple or green, closely matching the colors of other thin film structures in pigeon feathers, fly wings or butterfly scales.[49–51] The third mechanism is multilayer interference, which creates bright red-metallic elytra. The presence of multilayers is corroborated by both SEM data and reflectance spectra (Figure 5F,I). Note that there is no clear phylogenetic relationship between the elytron coloration mechanism and the color of the species (Figure 6). These mechanisms for elytral color generation have previously been reported in numerous beetle species[4,5] and their development has also been described.[52] From our studies, it appears that multilayers are only used to create red elytra, whilst other elytral colors are created by thin film interference.

The elytral colors can be related to geography, as found in the *Phelotrupes auratus* beetles.[53] The variation of *Pachyrhynchus* species with different elytral mechanisms, for example, in *P. erichsoni* (Figure 6) make similar geographic correlations unlikely. Although the exact function of the elytron color is unclear, by providing a background for the colored markings, it may aid in enhancing the color contrast for aposematic signaling.

3.5. Phylogenetic Studies

Our study shows no clear pattern within a clade relating to elytral color or PC structures within the scales (Figure 6). The data suggest that the scale structure, color, and the elytral color in *Pachyrhynchus* is not clustered in a particular clade. The differentiation of these traits within a particular species appears to vary as widely within a species group as between different groups, which confirm previous work by Van Dam et al.[26] We have identified the *P. congestus* and *P. orbifer* clades (Figure 6) to show vast variations in color, PC structure, elytral color, and domain size. The *P. orbifer* clade shows however no variation in PC type. As the domain size and PC type vary greatly between closely related species, this suggests that there is a common genetic pathway that is modified, perhaps in different ways, to produce the observed patterns.

4. Experimental Section

Samples: Specimens from two main entomology collections at the Coleoptera Research Center at the University of Mindanao and at the California Academy of Sciences were studied. (See Table S2, Supporting Information) for an overview of all investigated species.

Optical Characterization: Optical microscopy images were taken with a Point Grey Grasshopper 3 USB3 camera (GS3-U3-28S5C-C, Point Grey/FLIR Integrated Imaging Solutions Inc., Richmond, Canada), a Zeiss Axioskop A1 microscope (Zeiss AG, Oberkochen, Germany) and a Xenon light source (Thorlabs SLS401; Thorlabs GmbH, Dachau, Germany). A white diffuser standard was used as a reference. The microscope images of the scales were taken directly on the elytra of the various weevils.

Spectroscopy measurements were taken with a modified Zeiss Axioskop A1 (Zeiss AG, Oberkochen, Germany) and a photodiode spectrometer (Ocean Optics Maya2000 Pro; Ocean Optics, Dunedin, FL, USA). The reflectance/transmission spectra were taken with an optical fiber with a 230 µm core and spot size of 13 µm. Reflectance spectra were taken with a Zeiss Epiplan Neofluar 20 × (NA = 0.6) lens. Additionally and to assess reflectance peaks in the UV-wavelength range, that is, for *P., sanchezi*, reflectance spectra were measured with integrating sphere (AvaSphere-30, Avantes BV, Apeldoorn, Netherlands), connected with optical fibers to the Maya2000 Pro spectrometer and a balanced deuterium-halogen lamp (DH-2000-Bal; Ocean Optics, Dunedin, FL, USA). *k*-space measurements were performed using a Bertrand lens (Zeiss 453671) and a Zeiss Epiplan Neofluar 50× (NA = 0.9) objective.

To test for pigmentation, the scales of each specimen were scratched off their elytron onto a microscope glass slide using a needle. Transmission spectra of the scales were then measured with the above-mentioned light microscope. A drop of oil with a refractive index $n = 1.55$ (Series A, Cargille Labs, Cedar Grove, NJ, USA) was then placed on the slide and sandwiched with a cover slip. Transmission spectra of the scales immersed in oil were then measured.

Ultrastructure Analysis: Isolated scales were scratched off of the elytron with a needle onto an aluminium stub covered with carbon tape. This often removed part of the cortex of the scales, revealing the scale ultrastructure. The stubs were coated with ≈4–8 nm of gold to minimize charging effects, using a Cressington 208 HR sputter coater (Cressington Scientific Instruments, Watford, England). Copper tape and silver paste were added to the edges of the stubs to further reduce charging effects. These scales were then imaged with a Tescan Mira3 LM FE SEM (Tescan, Brno, Czechia) or a ThermoFisher Scios 2 DualBeam FIB-SEM (FEI, Eindhoven, the Netherlands). To study the domain size of certain scales, their outer cortex was removed in a 4:20 oxygen to argon plasma for 12–15 min, in a PE-100 RIE Benchtop Plasma Etching System (Plasma Etch Inc., Carson City, NV, USA). Measurements of the nearest neighbor distances and domain sizes from SEM images were conducted using Fiji (ImageJ 1.53c).[54] For quasi-ordered specimens, FFTs of the images was generated using Fiji. If the FFT of a quasi-ordered specimen was isotropic, that is, ring-shaped, the nearest neighbor distance was estimated by measuring the distance between the ring and the center.

To prepare cross-sections for SEM imaging, a focused ion beam (FIB) was used. The center of the scales were milled with ThermoFisher Scios 2 FIB, using a voltage of 30 kV and milling current varying from 0.01–1 nA. The SEM images were taken at 52° with activated tilt correction.

Ancestral State Reconstructions and Comparative Ultrastructure Analysis: To identify how often the four types of PCs (ordered, disordered, quasi-ordered, and quasi-ordered+ordered in the same individual) evolved within *Pachyrhynchus* the phylogenetic tree from[26] was used to map the structure data (Table S2, Supporting Information) onto the tree. The "fitMk" function of phytools v0.7.70[55] was used to reconstruct ancestral character states. The best fitting model was selected (equal rates ER, symmetric backward and forward rates SYM, all-rates-different for transitions ARD, or "transient," where the rates of gaining or losing polymorphic states were different), using the AIC weights as selection criteria. The models treated character transitions as unordered or ordered. After identifying the best fitting model (ER unordered), 1000 different character histories were simulated using the "make.simmap" function of phytools and the "mcmc" option to estimate the transition rate matrix, employing the best fitting model (see Table S3, Supporting Information).

To identify correlations between the optical properties of a certain nanostructure, the relationship of non-independence properties of the samples needs to be taken into account. To this end, the phylogenetically independent contrasts was calculated, using the pic function of the R package "ape."[56]

Statistical Analysis: Spectral measurements were taken from 7–15 different scales of each specimen. The reflectance spectra were then plotted on Origin 2016G software (OriginLabs) and the peak reflectance, peak wavelength, and FWHM measured for each individual spectrum. The resulting data is plotted as mean ± s.e.m.

The lattice parameters were measured from SEM images with around 20 measurements taken per sample with the use of Fiji (ImageJ 1.53c).[54]

The same software was used to measure the areas of different domains from top-view SEM images or cross-sectional FIB-SEM images. Here, the domain size was averaged from 1–3 different scales and 10–20 different domains. In certain cases, that is, *P. niitasoi* and *P. orbifer callainus*, the domain sizes were measured from optical microscopy data.

Model selection of the best fitting discrete character model of evolution, was assessed using the Akaike Information Criterion (AIC) model weights, where models that were overparameterized are down weighted. Analyses were conducted in the R package phytools v0.7.70. Phylogenetically independent contrasts were calculated using the "pic" function in the R package ape. Then, a linear model was fitted to the data and significance was assessed if the R-squared *P*-value was greater than 0.05.

Supporting Information

Supporting Information is available from the Wiley Online Library or from the author.

Acknowledgements

The authors thank Cedric Schumacher, Kenza Djeghdi, and Viola Bauernfeind for discussion and technical support. This study was supported by the European Research Council (ERC) through grant PrISMoID (833895). The authors further acknowledge financial support by the Adolphe Merkle Foundation, the National Science Foundation (1856402), and the Swiss National Science Foundation (SNSF) through the National Center of Competence in Research Bio-Inspired Materials and the Ambizione programme grant (168223).

Conflict of Interest

The authors declare no conflict of interest.

Author Contributions

A.P. and B.D.W. performed the measurements, B.D.W. and U.S. planned and supervised the work, A.P. processed the experimental data, performed the analysis, drafted the manuscript, and designed Figures 1– 5. M.V.D. performed the phylogenetic mapping and ancestral character states reconstruction and designed Figure 6. A.A.C. identified, collected, and provided a loan of the samples. B.D.W. and U.S. aided in interpreting the results and helped draft the manuscript. All authors edited and approved the final version of the manuscript.

Data Availability Statement

The research data that support the findings of this study are available at the Zenodo data repository (https://doi.org/10.5281/zenodo.6425390).

Keywords

biodiversity, biophotonics, color traits, diamond photonic crystals, order and disorder

Received: January 27, 2022
Revised: March 7, 2022
Published online:

[1] J. D. Joannopoulos, *Photonic Crystals: Molding the Flow of Light*, 2nd edn, Princeton University Press, Princeton, NJ **2008**.
[2] P. Vukusic, J. R. Sambles, *Nature* **2003**, *424*, 852.
[3] S. Kinoshita, S. Yoshioka, *ChemPhysChem* **2005**, *6*, 1442.
[4] D. G. Stavenga, B. D. Wilts, H. L. Leertouwer, T. Hariyama, *Philos. Trans. R. Soc. B: Biol. Sci.* **2011**, *366*, 709.
[5] D. G. Stavenga, *Mater. Today: Proc.* **2014**, *1*, 109.
[6] A. E. Seago, P. Brady, J.-P. Vigneron, T. D. Schultz, *J. R. Soc. Interface* **2009**, *6*, S165.
[7] B. D. Wilts, X. Sheng, M. Holler, A. Diaz, M. Guizar-Sicairos, J. Raabe, R. Hoppe, S.-H. Liu, R. Langford, O. D. Onelli, D. Chen, S. Torquato, U. Steiner, C. G. Schroer, S. Vignolini, A. Sepe, *Adv. Mater.* **2018**, *30*, 1702057.
[8] M. Burresi, L. Cortese, L. Pattelli, M. Kolle, P. Vukusic, D. S. Wiersma, U. Steiner, S. Vignolini, *Sci. Rep.* **2014**, *4*, 6075.
[9] K. Michielsen, D. G. Stavenga, *J. R. Soc. Interface* **2008**, *5*, 85.
[10] S. Yoshioka, H. Fujita, S. Kinoshita, B. Matsuhana, *J. R. Soc., Interface* **2014**, *11*, 20131029.
[11] B. D. Wilts, B. A. Zubiri, M. A. Klatt, B. Butz, M. G. Fischer, S. T. Kelly, E. Spiecker, U. Steiner, G. E. Schröder-Turk, *Sci. Adv.* **2017**, *3*, e1603119.
[12] V. Saranathan, S. Narayanan, A. Sandy, E. R. Dufresne, R. O. Prum, *Proc. Natl. Acad. Sci. U. S. A.* **2021**, *118*, e2101357118.
[13] B. D. Wilts, K. Michielsen, H. De Raedt, D. G. Stavenga, *J. R. Soc. Interface* **2012**, *9*, 1609.
[14] R. Ebihara, H. Hashimoto, J. Kano, T. Fujii, S. Yoshioka, *J. R. Soc. Interface* **2018**, *15*, 20180360.
[15] M. E. McNamara, V. Saranathan, E. R. Locatelli, H. Noh, D. E. G. Briggs, P. J. Orr, H. Cao, *J. R. Soc. Interface* **2014**, *11*, 20140736.
[16] S. Mouchet, J.-P. Vigneron, J.-F. Colomer, C. Vandenbem, O. Deparis, *Nat. Light: Light Nat. IV* **2012**, *8480*, 848003.
[17] C. T. Chan, K. Ho, C. Soukoulis, *Europhys. Lett.* **1991**, *16*, 563.
[18] B. A. Palmer, V. J. Yallapragada, N. Schiffmann, E. M. Wormser, N. Elad, E. D. Aflalo, A. Sagi, S. Weiner, L. Addadi, D. Oron, *Nat. Nanotechnol.* **2020**, *15*, 138.
[19] B. D. Wilts, B. Wijnen, H. L. Leertouwer, U. Steiner, D. G. Stavenga, *Adv. Opt. Mater.* **2017**, *5*, 1600879.
[20] K. Djeghdi, U. Steiner, B. D. Wilts, arXiv:2204.02228, **2022**.
[21] C. Pouya, D. G. Stavenga, P. Vukusic, *Opt. Express* **2011**, *19*, 11355.
[22] E. Bermúdez-Ureña, C. Kilchoer, N. P. Lord, U. Steiner, B. D. Wilts, *iScience* **2020**, *23*, 101339.
[23] M. D. Shawkey, V. Saranathan, H. Pálsdóttir, J. Crum, M. H. Ellisman, M. Auer, R. O. Prum, *J. R. Soc. Interface* **2009**, *6*, S213.
[24] L. Y. Wang, H. Rajabi, N. Ghoroubi, C. P. Lin, S. N. Gorb, *Front. Physiol.* **2018**, *9*, 1410.
[25] H.-Y. Tseng, C.-P. Lin, J.-Y. Hsu, D. A. Pike, W.-S. Huang, *Plos One* **2014**, *9*, e91777.
[26] M. H. Van Dam, A. A. Cabras, A. W. Lam, *bioRxiv 2020.12.18.422986* **2021**.
[27] V. Welch, V. Lousse, O. Deparis, A. Parker, J. P. Vigneron, *Phys. Rev. E* **2007**, *75*, 41919.
[28] J. W. Galusha, L. R. Richey, M. R. Jorgensen, J. S. Gardner, M. H. Bartl, *J. Mater. Chem.* **2010**, *20*, 1277.
[29] B. D. Wilts, V. Saranathan, *Small* **2018**, *14*, 1802328.
[30] Y. Chang, Y. Ogawa, G. Jacucci, O. D. Onelli, H. Y. Tseng, S. Vignolini, *Adv. Opt. Mater.* **2020**, *8*, 2000432.
[31] M. Saba, B. D. Wilts, J. Hielscher, G. E. Schröder-Turk, *Mater. Today: Proc.* **2014**, *1*, 193.
[32] B. D. Wilts, N. IJbema, K. Michielsen, H. De Raedt, D. G. Stavenga, *MRS Proc.* **2013**, *1504*, 803.
[33] R. K. Nagi, D. E. Montanari, M. H. Bartl, *Bioinspiration Biomimetics* **2018**, *13*, 35003.

[34] M. Y. Noh, S. Muthukrishnan, K. J. Kramer, Y. Arakane, *Curr. Opin. Insect Sci.* **2016**, *17*, 1.
[35] S. Magkiriadou, J. G. Park, Y. S. Kim, V. N. Manoharan, *Phys. Rev. E* **2014**, *90*, 062302.
[36] G. Jacucci, S. Vignolini, L. Schertel, *Proc. Natl. Acad. Sci. U. S. A.* **2020**, *117*, 23345.
[37] P. Vukusic, B. Hallam, J. Noyes, *Science* **2007**, *315*, 348.
[38] H. Ghiradella, *J. Morphol.* **1989**, *202*, 69.
[39] M. Stefik, S. Guldin, S. Vignolini, U. Wiesner, U. Steiner, *Chem. Soc. Rev.* **2015**, *44*, 5076.
[40] V. Saranathan, C. O. Osuji, S. G. Mochrie, H. Noh, S. Narayanan, A. Sandy, E. R. Dufresne, R. O. Prum, *Proc. Natl. Acad. Sci. U. S. A.* **2010**, *107*, 11676.
[41] H. Anbutsu, M. Moriyama, N. Nikoh, T. Hosokawa, R. Futahashi, *Proc. Nat. Acad. Sci. U. S. A.* **2017**, *114*, E8382.
[42] C. Y. Lee, S. P. Yo, R. W. Clark, J. Y. Hsu, C. P. Liao, H. Y. Tseng, W. S. Huang, *J. Zool.* **2018**, *306*, 36.
[43] D. E. Azofeifa, H. J. Arguedas, W. E. Vargas, *Opt. Mater.* **2012**, *35*, 175.
[44] H. L. Leertouwer, B. D. Wilts, D. G. Stavenga, *Opt. Express* **2011**, *19*, 24061.
[45] S. Yoshioka, S. Kinoshita, *Phys. Rev. E* **2011**, *83*, 051917.
[46] L. D. Bonifacio, B. V. Lotsch, D. P. Puzzo, F. Scotognella, G. A. Ozin, *Adv. Mater.* **2009**, *21*, 1641.
[47] C. E. Finlayson, A. I. Haines, D. R. E. Snoswell, A. Kontogeorgos, S. Vignolini, J. J. Baumberg, P. Spahn, G. P. Hellmann, *Appl. Phys. Lett.* **2011**, *99*, 261913.
[48] B. D. Wilts, K. Michielsen, J. Kuipers, H. De Raedt, D. G. Stavenga, *Proc. R. Soc. B: Biol. Sci.* **2012**, *279*, 2524.
[49] S. Yoshioka, E. Nakamura, S. Kinoshita, *J. Phys. Soc. Jpn.* **2007**, *76*, 13801.
[50] D. G. Stavenga, A. Matsushita, K. Arikawa, H. L. Leertouwer, B. D. Wilts, *J. Exp. Biol.* **2012**, *215*, 657.
[51] D. G. Stavenga, *Mater. Today: Proc.* **2014**, *1*, 109.
[52] O. D. Onelli, T. van de Kamp, J. N. Skepper, J. Powell, T. d. S. Rolo, T. Baumbach, S. Vignolini, *Sci. Rep.* **2017**, *7*, 1373.
[53] Y. Araki, T. Sota, *Mol. Ecol.* **2021**, *30*, 670.
[54] J. Schindelin, I. Arganda-Carreras, E. Frise, V. Kaynig, M. Longair, T. Pietzsch, S. Preibisch, C. Rueden, S. Saalfeld, B. Schmid, J.-Y. Tinevez, D. J. White, V. Hartenstein, K. Eliceiri, P. Tomancak, A. Cardona, *Nat. Methods* **2012**, *9*, 676.
[55] L. J. Revell, *Methods Ecol. Evol.* **2012**, *3*, 217.
[56] E. Paradis, J. Claude, K. Strimmer, *Bioinformatics* **2004**, *20*, 289.